Parameter Uncertainty Analysis of Common Infiltration Models

V. Clausnitzer, J. W. Hopmans,* and J. L. Starr

ABSTRACT

Water infiltration is a driving force influencing crop growth, soil erosion, and chemical leaching processes. Knowledge of the relative precision and accuracy of infiltration models is needed for best characterization of the infiltration parameters. The two-parameter Green–Ampt and Philip, three-parameter Horton, Mezencev, Swartzendruber, and Parlange et al., and four-parameter Barry et al. infiltration models were compared for their precision and accuracy of estimated parameter confidence intervals using simulated infiltration reference data. To account for potential levels of uncertainty, three levels of measurement error were included using a Monte Carlo analysis. Reference data were generated for a clay and a sandy loam soil using an adaptive-grid finite-element code. Results show that extending the measurement period provided parameter estimates with higher confidence, a more precise estimate of that confidence, and better defined minima in the objective function. The empirical Horton model resulted in the worst fits due to model bias, which also prevented estimation of parameter uncertainty for this model. The semianalytical Swartzendruber and the physically based Parlange et al. and Barry et al. models provided the best fits. Considering all selected criteria, the Swartzendruber model was a reasonable compromise under the conditions imposed in this study.

MANY APPROACHES have been presented to solve the problem of vertical infiltration of water into a homogeneous, semi-infinite soil. Youngs (1995) reviewed the historic development of infiltration theory including the classic solutions based on the Richards equation. Kutílek and Nielsen (1994, p. 140–159) presented a comprehensive review of analytical and empirical solutions. Typically, such parameterized solutions are fitted to measured infiltration data. The optimized parameters serve as a convenient, condensed description of the infiltration process. Moreover, model parameters can be used for predictive purposes, and physically based infiltration models allow estimation of soil hydraulic properties.

Prediction uncertainty, inherent in model simulations, needs to be estimated and reported. It is caused by errors due to violation of assumptions implicit in the model and by uncertainty in the model parameters. When obtaining parameters by fitting measured data, the error of the fitting model will in general be unknown, but the parameter uncertainty as caused by measurement errors can be estimated using confidence intervals. This uncertainty estimate is derived from the objective function in the vicinity of the optimized parameter set, and is statistically accurate for linear fitting models with zero model error and independent measurements of known uncertainty (Press et al., 1992, p. 663). In contrast, the true distributions of the optimized parameters are required to evaluate the accuracy of estimated confidence limits for nonlinear fitting models such as the investigated infiltration equations. These distributions can be obtained using the Monte Carlo method, whereby many realizations of optimized parameters sets are generated from model fitting of infiltration data with independent normally distributed measurement error.

Many factors may influence the selection of a model, including type of application, desired level of physical–mathematical rigor, and user preference. No single infiltration model can be expected to best meet all possible requirements simultaneously. Thus to be able to make an informed decision in a given case, knowledge of model performance under different criteria is desirable. The objective of this study was to compare infiltration equations in terms of precision and accuracy of estimated parameter confidence intervals. The effect of measurement time on infiltration model parameters and computational efforts were also compared. Specifically, we tested seven models for three different variances of simulated measurement errors. The considered infiltration models can be classified as empirical (Eq. [1] and [2]), semianalytical (truncated series solutions in Eq. [3] and [4]), or based on physical considerations (Eq. [5], [6], and [7]). The following presents the considered infiltration equations, which are also listed in Table 1 with their fitting parameters.

The empirical infiltration equation by Horton (1940) considers infiltration as a natural "exhaustion process", in which infiltration rate ($L\,T^{-1}$) decreases exponentially with time from a finite initial value, $\alpha_1 + \alpha_2$, to a final value, α_1. Accordingly, cumulative infiltration I (L) is predicted as a function of time t (HO model):

$$I = \alpha_1 t + \frac{\alpha_2}{\alpha_3}[1 - \exp(\alpha_3 t)] \qquad [1]$$

with $\alpha_3 > 0$. In Eq. [1], α_1 can be associated with the hydraulic conductivity ($L\,T^{-1}$) of the wetted soil portion, K_1, for $t \rightarrow \infty$. Another empirical model was proposed by Mezencev (1948), who modified the Kostiakov (1932) equation by including a linear term with a coefficient β_1, so that $\beta_1 \rightarrow K_1$ for $t \rightarrow \infty$, provided $0 < \beta_3 < 1$ and $\beta_2 > 0$ (ME model):

$$I = \beta_1 t + \frac{\beta_2}{1 - \beta_3} t(1 - \beta_3) \qquad [2]$$

Philip (1957a) presented an infinite-series solution to the water-content-based form of Richards' equation for the case of vertical infiltration. The solution converges to the true solution for small and intermediate times

V. Clausnitzer and J.W. Hopmans, Dep. of Land, Air and Water Resources, Univ. of California, Davis, CA 95616; and J.L. Starr, USDA-ARS, Beltsville, MD 20705. Received 29 Sept. 1997. *Corresponding author (jwhopmans@ucdavis.edu).

Published in Soil Sci. Soc. Am. J. 62:1477–1487 (1998).

Abbreviations: BA, Barry et al. model; GA, Green and Ampt model; HO, Horton model; LM, Levenberg–Marquardt; ME, Mezencev model; PA, Parlange et al. model; PH, Philip model; rms, root mean square; SW, Swartzendruber model.

Table 1. Infiltration model equations.

Model	Eq.	Abbreviation	Fitting parameters
Horton (1940)	[1]	HO	α_1, α_2, α_3
Mezencev (1948)	[2]	ME	β_1, β_2, β_3
Philip (1957c)	[3]	PH	A, S
Swartzendruber (1987)	[4]	SW	K_1, S, A_0
Green and Ampt (1911)	[5]	GA	K_1, G
Parlange et al. (1982)	[6]	PA	ΔK, S, δ
Barry et al. (1995)	[7]	BA	K_1, K_i, B_1, B_2

but fails for large times, for which case an alternative solution was presented (Philip, 1957b). With additional assumptions regarding the physical nature of soil water properties, Philip (1987) proposed joining solutions that are applicable for all times. Philip (1957c) introduced a truncation of the small-time series solution that is a simple two-parameter model equation (PH model):

$$I = At + St^{0.5} \quad [3]$$

"which should be accurate for all but very large t", and "suitable for applied hydrological studies". The sorptivity S (L $T^{-0.5}$) depends on several soil physical properties, including initial water content θ_i (L^3 L^{-3}) and the hydraulic conductivity and soil water retention functions. Because the coefficient A is not equal to K_1, physical interpretation of Eq. [3] fails for $t \rightarrow \infty$.

Swartzendruber (1987) proposed an alternative series solution that is applicable and exact for all infiltration times and also allows for surface ponding. Its simplified form is a three-parameter infiltration equation (SW model):

$$I = K_1 t + \frac{S}{A_0}[1 - \exp(-A_0 t^{0.5})] \quad [4]$$

and if $A_0 \rightarrow 0$, it reduces to a form of the Philip (1957b) model with K_1 as the coefficient of the linear term, and for which dI/dt approaches K_1 as $t \rightarrow \infty$.

The Green and Ampt (1911) model assumes an instantaneous change in water content at the wetting front from a uniform θ_i to the water content at natural saturation θ_1. The initial hydraulic conductivity, $K_i = K(\theta_i)$, is assumed to be zero. Moreover, the solution requires constant soil water pressure head (L) values at the surface, h_s, and at the wetting front, h_f. Applying Darcy's law, cumulative infiltration was expressed implicitly as (GA model)

$$I = K_1 t + (h_s - h_f)\,\Delta\theta \ln\left(1 + \frac{I}{(h_s - h_f)\,\Delta\theta}\right) \quad [5]$$

where $\Delta\theta$ is equal to $\theta_1 - \theta_i$. Defining $G = (h_s - h_f)\Delta\theta$, Eq. [5] can be used as a two-parameter model with fitting parameters K_1 and G. A related model (PA model) was proposed by Parlange et al. (1982):

$$t = \frac{S^2}{2(\Delta K)^2 (1 - \delta)}\left[2\frac{\Delta K}{S^2} I - \ln\frac{\exp\left(2\delta\frac{\Delta K}{S^2} I\right) + \delta - 1}{\delta}\right] \quad [6]$$

where ΔK is equal to $K_1 - K_i$. At the expense of a third parameter δ, Eq. [6] interpolates between the Green and Ampt approach and that of Talsma and Parlange (1972). The latter assumes a rapid change of the hydraulic conductivity K with water content θ, as opposed to the negligible rate of change in K at the wetting front implied by the original Green and Ampt model. As it is based on integration of the water-content-based form of Richards' equation, the theoretical scope of Eq. [6] is limited to nonponded conditions. In this study, Eq. [6] was applied to ponded conditions under the assumption that the positive surface pressure head will be accounted for by an increase in the sorptivity (Philip, 1958) relative to nonponded conditions. A generalization of Eq. [6] to include ponded conditions without affecting the value of S was introduced by Parlange et al. (1985). Haverkamp et al. (1988) demonstrated parameter time independence and superior prediction accuracy for the Parlange et al. (1985) model compared with the Kostiakov (1932), HO, ME, GA, and PH models. Subsequently, Haverkamp et al. (1990) presented a modification of their model to include upward water flow by capillary rise. The resulting infiltration model contains six physical parameters, in addition to the interpolation parameter δ, which may be set to unity for infiltration (Haverkamp et al., 1990). Both the PA and the Haverkamp (1990) model require an iterative procedure to predict $I(t)$. Barry et al. (1995) presented an explicit approximation to the Haverkamp et al. (1990) model, retaining all six physical parameters (BA model):

$$I = K_i t + \frac{S^2 + 2K_1 h_s \Delta\theta}{2\Delta K}\left(t^* + 1 - \gamma - \exp\left(\frac{-6(2t^*)^{0.5}}{6 + (2t^*)^{0.5}} - \frac{2t^*}{3}\right) + \frac{\gamma}{1 + t^*}\left\{\exp\left(-\frac{2t^*}{3}\right)[1 - (1 - \gamma)^8\, t^{*2.5}] + (2\gamma + t^*)\ln\left(1 + \frac{t^*}{\gamma}\right)\right\}\right) \quad [7]$$

where

$$t^* = \frac{2t(\Delta K)^2}{S^2 + 2K_1 h_s \Delta\theta}$$

$$\gamma = \frac{2K_1(h_s + h_a)\Delta\theta}{S^2 + 2K_1 h_s \Delta\theta}$$

and h_a denotes the absolute value of the soil water pressure head at which the air phase becomes discontinuous after wetting. Defining

$$B_1 = (h_s + h_a)\Delta\theta$$

and

$$B_2 = \frac{2}{S^2 + 2K_1 h_s \Delta\theta}$$

Eq. [7] can be expressed using only four fitting parameters: K_i, K_1, B_1, and B_2.

If infiltration measurements are complemented with estimates of volumetric water content, surface soil water potential, or hydraulic conductivity values, the number of fitting parameters in the nonempirical models could theoretically be reduced. However, most such measurements have high uncertainties associated with them so that their knowledge prior to fitting would not necessar-

ily result in improved estimates for the remaining physical fitting parameters. In addition, assumptions made in the model development are typically violated. For example, field soils are generally heterogeneous and θ_i, θ_l, and K_l are not constant with depth. Therefore, when applied to field-measured infiltration data, the semianalytical and physically based models are often fitted without necessarily considering the physical significance of their parameter values. In treating all parameters as effectively empirical, their fitted values are not expected to always reflect physical conditions, particularly in cases when the number of fitting parameters is large. Therefore, in this study each model's parameter vector was considered a priori unknown and subjected to the fitting procedure. When applicable, fitted saturated hydraulic conductivity and sorptivity values were compared with their theoretical values.

METHODS

Reference Infiltration Data

Reference data, free of measurement errors, are needed to generate infiltration data with controlled "measurement" errors. For this purpose, true cumulative infiltration (I) as a function of time t (T) was calculated using a one-dimensional numerical scheme solving Richards' equation:

$$\frac{d\theta}{dt}\frac{\partial h}{\partial t} = \frac{\partial}{\partial z}\left[K\left(\frac{\partial h}{\partial z} + 1\right)\right] \quad [8]$$

where z (L) denotes the vertical space coordinate (positive upward). Assumptions inherent in the simulations include a rigid homogeneous medium, isothermal conditions, and a continuous air phase at atmospheric pressure.

The hydraulic properties of a given soil control the shape of the respective infiltration curve; in particular, the time of approaching steady state and the value of the steady-state slope. To cover a broad range of the soil hydraulic spectrum, reference data were obtained for a sandy loam and for a clay. For each soil, $I(t)$ reference data sets for a 5- and a 20-h period were simulated and represented by 70 and 140 (I, t) points, respectively. Points were selected so as to be equally spaced on a $t^{0.5}$ axis, thus providing the highest density of cumulative infiltration data near the origin. The two periods of distinctively different length (5 and 20 h) were chosen to identify the effect, if any, of the later part of the curve on the goodness of fit and on the size of confidence intervals for the optimized infiltration equation parameters. In addition, it allowed comparison of optimized parameters between long and short sets to identify time dependence of the parameters.

Soil water retention and conductivity curves were assumed to be described by the van Genuchten (1980) relationships:

$$\Theta = \begin{cases} [1 + (-ah)^n]^{-m} & h < 0 \\ 1 & h \geq 0 \end{cases} \quad [9a]$$

$$m = 1 - \frac{1}{n} \quad [9b]$$

$$K = K_s\Theta^l [1 - (1 - \Theta^{1/m})^m]^2 \quad [9c]$$

where h is the soil water pressure head, and a (L^{-1}), n, and l are fitting parameters, K_s (L T^{-1}) is the saturated hydraulic conductivity, and Θ is the normalized effective volumetric water content, defined as

$$\Theta = \frac{(\theta - \theta_r)}{(\theta_s - \theta_r)} \quad [9d]$$

with θ_r and θ_s denoting residual and saturated volumetric water content (L^3 L^{-3}), respectively. Using data given by van Genuchten (1980), θ_r, θ_s, a, n, K_s, and l were set equal to 0.0 m^3 m^{-3}, 0.446 m^3 m^{-3}, 0.152 m^{-1}, 1.17, 3.417 × 10^{-5} m h^{-1}, and 0.5, respectively, for the clay soil. For the sandy loam, the hydraulic parameters were 0.1346 m^3 m^{-3}, 0.3213 m^3 m^{-3}, 1.74 m^{-1}, 1.8646, 3.5125 × 10^{-3} m h^{-1}, and −0.4509, respectively (Wendroth et al., 1993).

Infiltration was simulated with soils initially in hydraulic equilibrium, using soil water pressure head values of −5 and −15 m at the soil surface for the sandy loam and clay soils, respectively, and constant-head boundary conditions at the top and bottom of the modeled spatial domain. The surface ponding depth, h_s, was set to 5 cm for both soil types. A hydraulic equilibrium initial condition required a soil depth of 15 m for the clay and 5 m for the sandy loam soil, so that the soil water pressure head at the bottom was zero, simulating a stationary groundwater table. Moreover, the chosen initial and boundary conditions ensured approximately uniform initial water content with the initial volumetric water content increasing <1 volume percent throughout the wetted soil depth.

The solution $h(z, t)$ was obtained from a finite-element, Picard time-iterative model using linear elements and a Galerkin formulation at each time step. Plots of $\theta(z, t)$ are presented in Fig. 1a and 1b. Standard fixed-grid algorithms such as HYDRUS (Kool and van Genuchten, 1991) were unable to prevent numerical instabilities in the simulated pressure-head curves due to the extreme head gradients in these simulations.

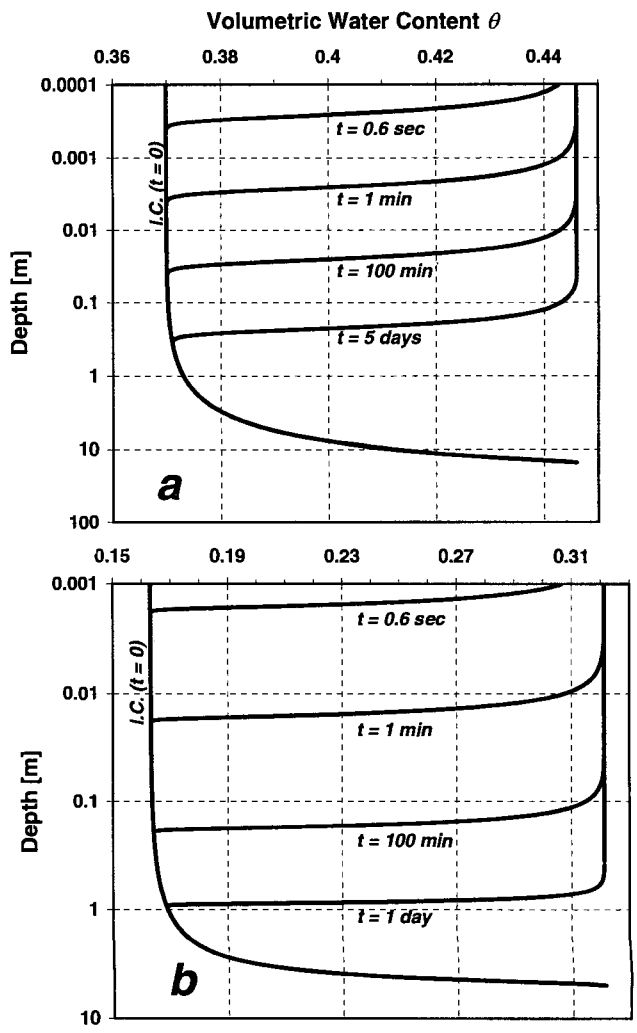

Fig. 1. Infiltration profiles for (a) clay and (b) sandy loam soils.

Thus, an adaptive-grid algorithm was developed that periodically recreates the finite-element grid, depending on the position of the wetting front, to maintain the highest node density in those portions of the $h(z)$ curve where $|\partial^2 h/\partial z^2|$ is maximal. Consequently, the number of grid nodes changes during a simulation. For the cases presented here, it was on the order of 1000 at all times. Total mass balance errors were 1.83 and 0.73% for the sandy loam and clay simulations, respectively. The adaptive-grid finite-element Richards Equation Solver RES-1D, written in C for UNIX, will be documented and released into the public domain (Clausnitzer, 1998, unpublished data).

Infiltration Model Equations

The seven selected infiltration equations are listed in Table 1, together with their respective two-letter abbreviations and list of fitting parameters. Both the GA and the PA models are nonexplicit expressions requiring iterative solutions in t for each I to be predicted. Since cumulative infiltration grows monotonically with time, a bisection method was employed in both cases to find the value of I whose argument t matches the time for which the respective prediction is to be made. The iterative nature of the bisection process causes an increase in computational cost by one or several orders of magnitude, depending on the desired accuracy.

Provided that the assumptions of a nonempirical model are valid for a given soil, the question arises whether the fitted physical parameters of those models represent the real soil hydraulic parameters. In the context of this study, we asked whether the fitted infiltration-model parameters reproduce the hydraulic conductivity and sorptivity values used in the finite-element simulations to generate the reference infiltration data. In our analysis, the results of this comparison might indeed depend on the hydraulic model selected.

The hydraulic conductivity of the wetted soil portion appears as parameter K_1 in the GA, SW, and BA models. Because a positive head was applied at the surface, K_1 for the reference simulations is equal to K_s. In the PA model, the parameter ΔK is the difference between K_1 and K_i. Given the dry initial condition used in these simulations, the initial conductivity can be neglected compared with K_s.

The sorptivity appears directly as a fitting parameter in the PH, PA, and SW models, and can be isolated as $(2K_1G)^{0.5}$ and $(2/B_2 - 2K_1h_s\Delta\theta)^{0.5}$ from the fitted values of G and B_2 for the GA (Haverkamp et al., 1988) and BA models, respectively. In the BA model, S is not affected by surface ponding, which is explicitly accounted for by h_s; for the other models, S depends on the pressure head at the surface. From Philip's (1957a,c) definition of S, it follows that $I = St^{0.5}$ for horizontal infiltration, with the numerical value of I at $t = 1$ equal to that of S. To obtain theoretical sorptivity values for the GA, PA, PH, and SW models, horizontal infiltration was simulated, using RES-1D, until $t = 1$ min for each soil with applied conditions similar to the respective vertical case. Simulations were performed with a zero-head condition applied at the surface to obtain the theoretical S values for the BA model.

Optimization Algorithm

Parameter optimization was performed by squared-residual minimization using the program LM-OPT (Clausnitzer and Hopmans, 1995), an implementation of the Levenberg–Marquardt (LM) algorithm. The LM algorithm combines the standard steepest-descent and quadratic-extrapolation minimization methods using a dimensionless parameter λ, which is updated after each iteration. The λ-updating procedures in LM-OPT are extensions of the standard LM-procedure, aimed at improving efficiency by reducing the number of iterations needed to reach convergence at an optimum.

In this study, LM-OPT was used to minimize the objective function q, defined as the sum of normalized residuals according to

$$q = \sum_{i=1}^{N} \frac{r_i^2}{\sigma^2(I_i)} \qquad r_i = I_i - I(t_i, \mathbf{p}) \qquad [10]$$

where t_i, I_i, r_i, and $\sigma^2(I_i)$ denote time, cumulative infiltration, residual, and measurement variance, respectively, for data point i. The total number of data points is N. The predicted cumulative infiltration is obtained from the model function $I(t_i, \mathbf{p})$ utilizing the parameter vector $\mathbf{p}$, which is different for each of the infiltration equations of Table 1. Dividing r_i^2 by $\sigma^2(I_i)$ accomplishes normalization by making q values dimensionless and thus more suitable for comparison. Final fits will be reported as root mean square, rms, defined as

$$\text{rms} = \sqrt{\frac{q}{N}} \qquad [11]$$

Each optimization was terminated if the relative improvement in q between iterations was <0.001.

To compare minimization algorithms, all optimizations were also performed using the line-search-based Rosenbrock (Bazaraa et al., 1993) and Powell (Press et al., 1992) methods. The LM procedure in all cases arrived at the objective-function minimum using a number of objective function evaluations about one order of magnitude lower than either line-search method. Therefore, all results reported are those obtained using the LM method.

Monte Carlo Analysis and Parameter Distributions

"Measured" data sets were generated from each of the reference sets by imposing normally distributed, independent "measurement" errors in I for the $I(t)$ reference data (Fig. 2). To identify the effect of the magnitude of the measurement errors, three values for the standard deviation of the imposed errors, σ_E, were chosen for each soil. The largest error level was defined so that for any two adjacent data points $I(t_i)$ and $I(t_{i+1})$, $I(t_i) + \sigma_E$ would be approximately equal to $I(t_{i+1}) - \sigma_E$. Accordingly, σ_E values of 0.007, 0.014, and 0.021 mm were chosen for the clay, and 0.1, 0.2, and 0.3 mm for the sandy loam soil. We will hereafter refer to these error levels as small, medium, and large, respectively. Five thousand data sets were generated for each reference set and error level. Subsequent analysis showed that this number was statistically sufficient, since different groups of 5000 generated data sets produced near-identical results. Figures 2a and 2b show the reference infiltration data sets with large σ_E for the clay and sandy loam soils, respectively.

Setting the variance value, $\sigma^2(I_i)$, equal to the square of the respective σ_E value, each model equation was fitted to each of the error-imposed data sets. Thus, 5000 optimized parameter sets were obtained for each model equation and combination of infiltration reference data and error level for a total of $7 \times 4 \times 3$ cases. Initial parameter estimates for fitting the error-imposed data sets were obtained by fitting each model equation to the respective reference curve first.

For an appropriate model, we can assume that all uncertainty in the parameters is due to uncertainty in the data. Denoting the variance of the measured value I_i by $\sigma^2(I_i)$, the parameter variance in a general linear model is given by

$$\sigma^2(p_j) = \sum_{i=1}^{N} \sigma^2(I_i) \left(\frac{\partial p_j}{\partial I_i}\right)^2 \qquad [12]$$

For a linear model and normal independent measurement

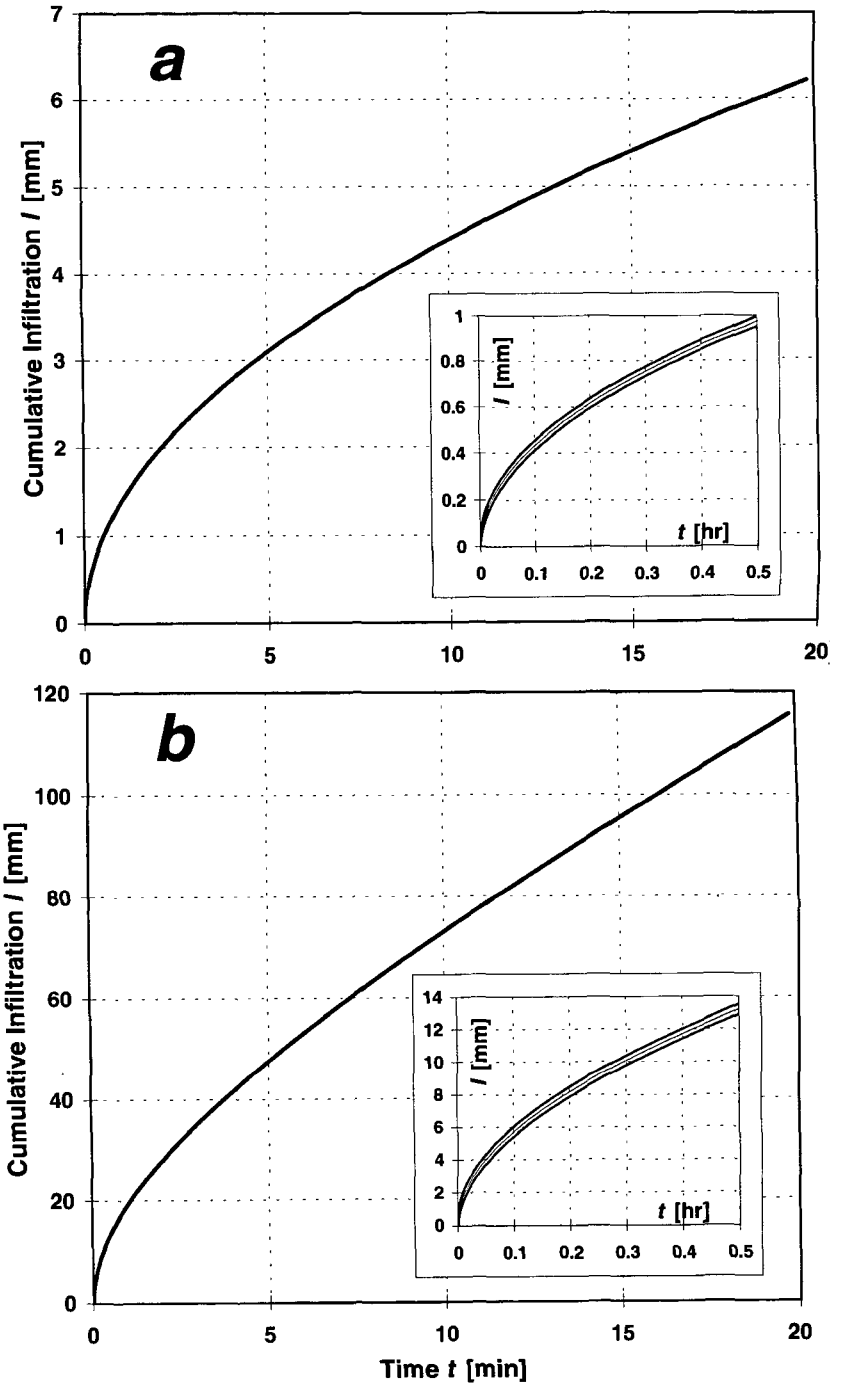

Fig. 2. Cumulative infiltration as a function of time; reference data for (a) clay and (b) sandy loam soils. Inserts show cumulative infiltration (I) as a function of time (t) for the imposed largest standard deviation (σ_E) of the error bounds.

errors, the distribution of an individual parameter p_j will also be normal and thus its 95.4% confidence interval will be given by $\pm 2\sigma(p_j)$ (Press et al., 1992, p. 696). We can assume that this also holds for nonlinear infiltration models as long as the $\sigma^2(I_i)$ values are reasonably small, in addition to being normal and independent. Otherwise stated, the predicted parameter confidence interval should not extend beyond the range for which a first-order approximation (as in a truncated Taylor-series expansion about the parameter optimum) of the model equation is applicable at each data point. Based on this assumption, the standard deviations for all optimized parameters are estimated in LM-OPT as

$$\sigma(p_j) = (\mathbf{B}_{jj})^{0.5} \qquad [13]$$

where the matrix **B** is the inverse of matrix **A** with elements A_{jk} given by

$$A_{jk} = \sum_{i=1}^{N} \frac{1}{\sigma^2(I_i)} \frac{\partial I(t_i, \mathbf{p})}{\partial p_j} \frac{\partial I(t_i, \mathbf{p})}{\partial p_k} \qquad [14]$$

evaluated at the optimum. The off-diagonal terms in **B** are the estimated local parameter-covariance values. For a detailed treatment including proof of equivalency of Eq. [14] and [12], see Clausnitzer and Hopmans (1995).

To test the usefulness of the local-linearity assumption for the different models, the average predicted 95.4% confidence intervals for each case using Eq. [13] were compared with the corresponding actual interval encompassing 95.4% of all 5000

Table 2. Final root mean square values for reference infiltration data.

Model	Clay		Sandy loam	
	5 h	20 h	5 h	20 h
	μm			
Green and Ampt	1.16	5.63	22.0	185
Philip	0.131	0.325	30.9	262
Horton	64.1	128	808	1520
Mezencev	0.043	0.324	13.0	110
Parlange et al.	0.135	0.317	0.516	8.49
Swartzendruber	0.131	0.315	1.69	17.1
Barry et al.	0.171	0.411	0.809	10.8

optimized parameter values. The latter was computed as the difference between the largest and smallest parameter value that remained after excluding 2.3% at both ends of the respective parameter distribution. The Kolmogorov–Smirnov test was applied to check for normality of the parameter distribution.

RESULTS AND DISCUSSION

Model Precision

Reference Data Sets

Since the reference infiltration data have no imposed "measurement" error, the variance in Eq. [10] was set to unity, yielding rms values that have the same units as I (Table 2). Moreover, these rms values represent a direct measure of systematic model error, or bias. Due to the difference in cumulative infiltration, the final rms for the sandy loam is larger than that of the clay for the same duration of infiltration. The HO model resulted in the worst fit in all cases, with rms values larger by several orders of magnitude than the other models in the case of the clay. Only the nonempirical three-and four-parameter models (PA, SW, and BA) resulted in excellent fits to all four reference sets. However, the PA, SW, and, in particular, BA models required a trial-and-error approach for the initial parameter values due to optimum nonuniqueness. Figure 3 shows the residuals for the fitted 20-h reference data, together with the "large" imposed error level for each soil.

Monte Carlo Data Sets

A more general comparison of model bias is possible using the Monte Carlo results. Average final rms values using all 5000 sets are given in Table 3. For an appropriate (i.e., unbiased) model, the average rms should be close to unity in all cases due to the normalization of the residuals with respect to the standard deviation of the measurement errors (Eq. [10]). That is, for an unbiased infiltration model, the average squared residual is approximately equal to the error variance. Any final rms values greater than unity indicate bias. In particular, all values that are underlined have <1% probability of representing an unbiased model, using the standard χ^2 test. The rms contribution from bias is numerically amplified by decreasing "measurement" errors (σ_E values). Evidently, the HO model gave rise to a substantial systematic error for both investigated soils and had to be considered an unsuitable model for the considered data. The HO model was excluded from further analysis because the subsequent computation of confidence intervals is meaningful only for unbiased models.

For the clay data, none of the remaining six models showed any bias for the 5-h set, and only the GA model exhibited bias for the 20-h set. As Table 3 and Fig. 3b show, both two-parameter models (GA and PH) and the ME model lacked the flexibility to provide an unbiased fit to the 20-h sandy loam data. For the PH model, this may indicate that the large time limit of applicability was reached in this case. The PA, SW, and BA models had negligible bias in all cases.

Confidence Intervals for Optimized Parameters

Actual Width of Confidence Intervals

The values in Table 4 represent the width of the 95.4% confidence intervals obtained by excluding 2.3% at both ends of the respective distribution of 5000 optimized parameters for each case. To permit comparison, each interval length was divided by the value of the respective mean parameter value. Underlined values denote cases where the 95.4% confidence interval is larger than 10% of the numerical value of the mean.

A large parameter confidence interval can be caused either by low relative sensitivity of the objective function to the respective parameter in the vicinity of the optimum (i.e., a relatively "flat" objective function in that particular parameter direction, represented by numerically small $\partial I_i/\partial p_j$ values), or by the existence of several distinct local minima (nonuniqueness). In the latter case the individual confidence intervals corresponding to each minimum appear together as one "effective" overall confidence interval. Either case represents a complication for parameter estimation. In contrast, small actual confidence intervals as obtained by a Monte Carlo procedure indicate well-behaved objective functions favorable to rapid convergence of the minimization algorithm.

As expected, confidence intervals grow as the magnitude of the "measurement" error, i.e., the uncertainty in the data, increases. Of perhaps greater practical importance is the fact that, in nearly all cases, better defined parameter optima were obtained by including more data in the optimization. The single exception, the BA model's K_i parameter in the case of the sandy loam data, may be caused by several local minima probably due to the high dimensionality of the parameter space for this model. Better defined optima are indicated by smaller confidence intervals, reflecting the reduced overall uncertainty due to the additional "measurements". In mathematical terms, the magnitude of $\partial p_j/\partial I_i$ in Eq. [12] decreases as the number of measured values increases. More data can be included either by increasing measurement density in time (results not shown here) or by extending the measurement period from 5 to 20 h. The effect of both was tested individually using the 5-h data sets. Increasing the measurement density by a factor of two always resulted in a smaller reduction of the confidence intervals than doubling the measurement period (on a $t^{0.5}$ scale), even though in both cases the number of data points was doubled. In

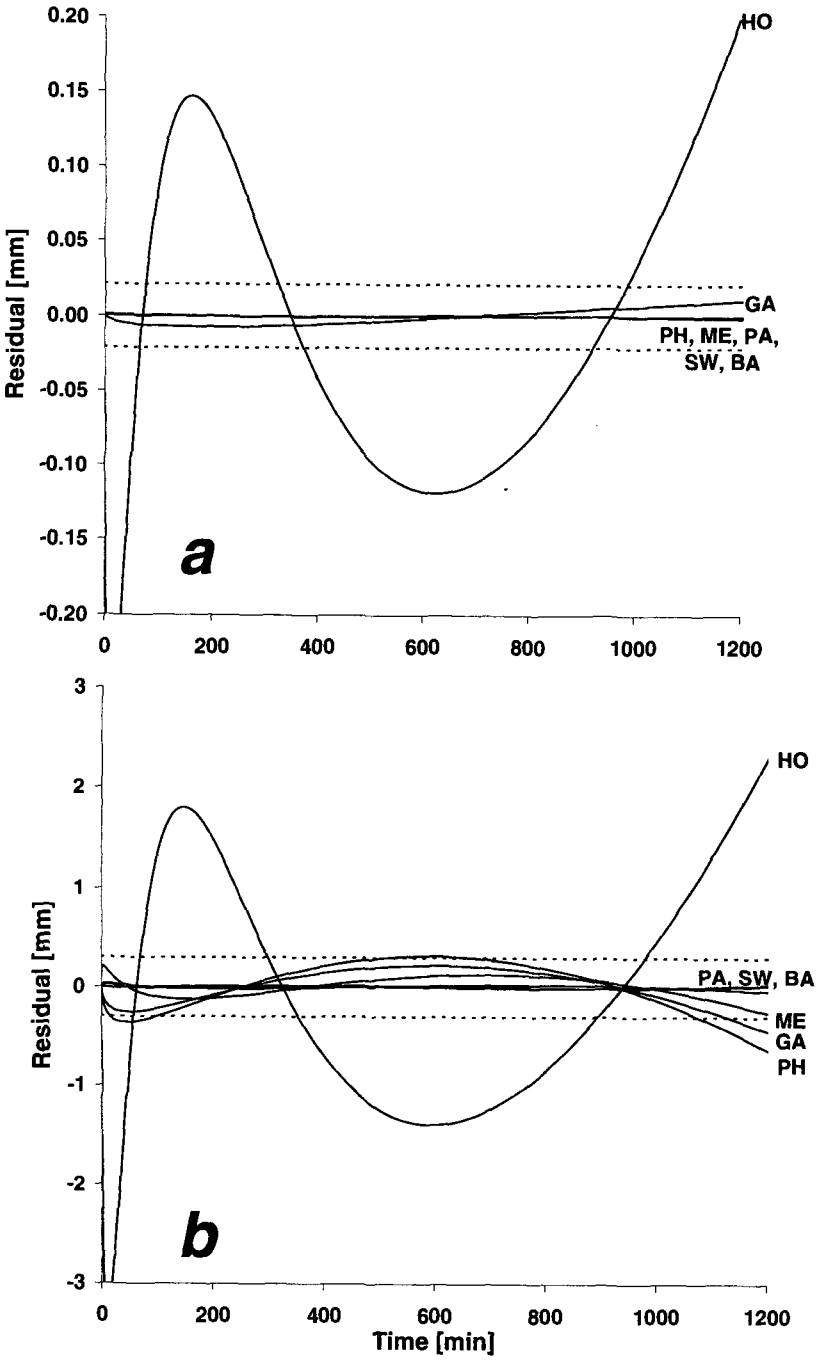

Fig. 3. Residuals for each model's fit of the 20-h reference data for (a) clay and (b) sandy loam soils. Dotted lines indicate the imposed errors, $\pm\sigma_E$, for the respective "large" error level.

particular, the 20-h confidence intervals of the sandy loam soil (Table 4) show the beneficial effect of extended infiltration measurements. A reduction in confidence interval by increasing the measurement period was not as clear for the clayey soil, indicating a possible texture effect. Except for the BA model, this latter data set provided the only case with small σ_E, where the confidence-interval width did not exceed 10% of the respective mean for any parameter. Table 4 also shows that increasing the number of parameters does not necessarily cause increased parameter uncertainty, as experience might suggest. In those cases where it does (e.g., several models for the 5-h clay data and BA model for sandy loam data), it is important to recognize that increased parameter uncertainty does not prevent an improvement in goodness of fit. Uncertainty is related to the curvature of the objective function at the optimum, while goodness of fit is measured by the value of the objective function.

Accuracy of Confidence-Interval Prediction

The ratio between *average predicted* width and the *actual* width of each 95.4% confidence interval was de-

Table 3. Average final root mean square values for small (sm), medium (md), and large (lg) imposed errors (σ_E) using all 5000 sets; underlined values have <1% probability of representing an unbiased model.

	Clay						Sandy loam					
	5 h			20 h			5 h			20 h		
Model	sm	md	lg	sm	md	lg	sm	md	lg	sm	md	lg
Green and Ampt	1.004	0.993	0.992	1.278	1.072	1.029	1.007	0.989	0.986	2.101	1.355	1.167
Philip	0.982	0.982	0.982	0.991	0.991	0.990	1.029	0.994	0.987	2.803	1.642	1.320
Horton	9.211	4.683	3.205	18.372	9.227	6.196	8.142	4.158	2.864	15.208	7.653	5.156
Mezencev	0.975	0.975	0.975	0.989	0.988	0.988	0.984	0.977	0.976	1.478	1.130	1.053
Parlange et al.	0.980	0.979	0.980	0.993	0.992	0.992	0.977	0.978	0.979	0.991	0.988	0.988
Swartzendruber	0.984	0.985	0.986	0.991	0.990	0.990	0.976	0.976	0.977	1.002	0.991	0.989
Barry et al.	0.984	0.984	0.984	0.995	0.993	0.993	0.975	0.976	0.977	0.990	0.987	0.988

termined, for each model parameter and all considered cases, as a measure of the accuracy of the parameter standard deviations predicted by Eq. [13]. Each average predicted width was obtained from the respective set of 5000 confidence intervals. The average accuracy in the predicted width of the 95.4% confidence interval improves as the value of the respective ratio, given in Table 5, approaches unity. Ratios close to unity provide support for the local-linearity assumption. In contrast, a large deviation from unity indicates a strong local nonlinearity in the respective parameter, unpredictability of parameter confidence due to nonuniqueness, or both.

The Kolmogorov–Smirnov test showed that all parameter distributions were nonnormal at the 0.01 significance level, i.e., with a 0.01 probability that a normal distribution would not be recognized as such. Nevertheless, a large number of the confidence-interval predictions in Table 5 were accurate for practical purposes, assuming a 10% error as acceptable. The PH and ME models appeared unaffected by the duration of the measured period and provided consistently acceptable confidence estimates for the small and medium error levels, except for the 20-h sandy loam data, where both models had shown bias (Table 3). For all other models, prediction accuracy was considerably higher for sandy loam than for clay data, and for 20- than for 5-h data. The only exception, the GA model applied to the 20-h sandy loam data, again corresponds to model bias. The values in Table 5 suggest that the PH and ME models have a relatively low nonlinearity associated with their parameters in general, while for the 20-h sandy loam data, both the PA and the SW model have become sufficiently linear in all parameters to permit useful confidence estimates even for the large error level. The fact that confidence estimates for the parameters of the BA model do not attain this level of accuracy may be an indication of nonunique parameter optima. For the two- and three-parameter models, all average predicted parameter confidence intervals that were inaccurate by 5% or more were wider than the corresponding actual confidence interval, and thus conservative. However, results for the clay data show that several models may grossly overestimate confidence intervals if the measurement period is short.

When estimating the parameter confidence intervals using Eq. [13], it is implied that model parameters are

Table 4. Actual width of 95.4% confidence intervals for small (sm), medium (md), and large (lg) imposed errors (σ_E) expressed as a multiple of the respective mean optimized parameter; values >0.1 underlined.

		Clay						Sandy loam					
		5 h			20 h			5 h			20 h		
Model	Parameter	sm	md	lg	sm	md	lg	sm	md	lg	sm	md	lg
Green and Ampt	K_1	0.003	0.006	0.011	0.001	0.002	0.003	0.044	0.089	0.133	0.005	0.012	0.018
	G	0.001	0.002	0.003	0.0005	0.0008	0.001	0.060	0.120	0.177	0.009	0.022	0.034
Philip	A	1.103	2.112	2.574	0.207	0.414	0.622	0.050	0.100	0.149	0.005	0.014	0.022
	S	0.007	0.014	0.020	0.003	0.005	0.008	0.008	0.017	0.025	0.002	0.006	0.009
Mezencev	β_1	5.175	10.580	16.500	0.791	1.588	2.401	0.169	0.339	0.513	0.018	0.039	0.060
	β_2	0.010	0.019	0.029	0.008	0.016	0.023	0.011	0.021	0.032	0.008	0.017	0.025
	β_3	0.022	0.044	0.066	0.008	0.015	0.023	0.024	0.048	0.072	0.007	0.016	0.024
Parlange et al.	ΔK	0.769	1.199	1.543	0.101	0.197	0.300	0.281	0.337	0.360	0.018	0.037	0.056
	S	0.006	0.012	0.018	0.002	0.004	0.006	0.014	0.020	0.027	0.006	0.013	0.019
	δ	0.633	0.913	1.138	0.067	0.136	0.208	0.641	0.781	0.802	0.088	0.178	0.268
Swartzendruber	K_1	0.331	0.659	1.025	0.080	0.161	0.244	0.359	0.570	0.683	0.020	0.041	0.061
	S	0.005	0.009	0.014	0.003	0.006	0.008	0.022	0.038	0.052	0.008	0.017	0.025
	A_0	3.825	4.582	5.212	0.130	0.259	0.390	0.901	1.423	1.698	0.076	0.154	0.232
Barry et al.	K_1	0.050	0.113	0.174	0.006	0.012	0.017	0.088	0.134	0.164	0.020	0.041	0.042
	K_i	0.059	0.136	0.220	0.015	0.031	0.048	2.112	3.508	5.723	2.585	5.099	6.614
	β_1	1.518	1.898	1.994	1.222	1.156	1.296	1.300	1.348	1.407	0.192	0.799	0.826
	β_2	0.002	0.005	0.009	0.001	0.001	0.002	0.014	0.026	0.037	0.006	0.012	0.018

Table 5. Ratio between estimated and actual width of 95.4% confidence intervals for small (sm), medium (md), and large (lg) imposed errors (σ_E).

		Clay						Sandy loam					
		5 h			20 h			5 h			20 h		
Model	Parameter	sm	md	lg	sm	md	lg	sm	md	lg	sm	md	lg
Green and Ampt	K_1	236.1	232.3	227.9	119.8	118.4	126.3	1.059	0.057	1.057	1.265	1.082	1.073
	G	242.7	228.5	223.4	99.52	99.32	113.1	1.007	1.007	1.020	1.266	1.061	1.056
Philip	A	1.006	1.045	1.239	0.992	0.992	0.992	1.006	1.006	1.006	1.380	1.027	1.023
	S	1.008	1.047	1.153	1.007	1.007	1.001	1.008	1.009	1.008	1.445	1.041	1.027
Mezencev	α_1	1.022	1.019	1.020	1.054	1.055	1.053	1.029	1.027	1.022	1.184	1.077	1.080
	α_2	1.018	1.018	1.019	1.045	1.044	1.043	1.022	1.022	1.021	1.175	1.077	1.085
	α_3	1.038	1.039	1.041	1.052	1.054	1.054	1.042	1.042	1.044	1.181	1.076	1.109
Parlange et al.	ΔK	13.10	15.68	17.89	8.671	8.928	8.832	1.424	2.767	3.864	0.988	0.984	0.960
	S	2.747	2.537	2.519	3.188	3.199	3.126	1.452	1.918	2.222	1.061	1.053	1.026
	δ	30.13	42.77	52.24	29.96	29.89	29.74	1.528	3.104	4.512	1.033	1.031	1.016
Swartzendruber	K_1	59 360	59 680	65 360	114.6	114.6	113.7	1.018	1.563	2.721	1.053	1.048	1.045
	S	3.706	3.995	4.119	2.482	2.494	2.494	1.035	1.182	1.299	1.037	0.036	1.026
	A_0	61 280	62 140	67 100	117.4	117.7	117.6	1.022	1.488	2.334	1.054	1.048	1.039
Barry et al.	K_1	207.8	215.0	201.9	301.8	306.6	3.106	6.016	15.22	42.35	0.817	1.662	2.334
	K_i	987.1	795.0	688.8	43.13	41.09	43.27	10.79	20.92	41.87	1.077	1.345	1.375
	β_1	1 598	1 350	1 124	656.8	298.4	222.2	35.86	1 601	2 741	0.832	1.730	2.551
	β_2	1 607	1 289	1 124	68.01	66.75	68.61	1.737	2.041	2.272	1.064	1.298	1.341

independent. This adds a safety margin to the estimated prediction uncertainty because correlation between model parameters in the vicinity of the optimum reduces the applicable domain in parameter space from which to predict parameter sets. Indeed, the optimized parameters were found to be (locally) strongly correlated in nearly all cases. This may explain why extending the measurement period reduced the uncertainty not only of the conductivity parameter, but of most other parameters as well. Figure 4 shows a plot of the 5000 optima obtained by fitting the PH model to the 20-h clay data with large σ_E. Plots for medium and small σ_E were identical except for proportionally smaller parameter ranges on both axes. The correlation structure for the PH model in Fig. 4 was typical for all considered models, and patterns of correlation between parameters were similarly shaped for the other infiltration models (in particular those for the 20-h sandy loam data).

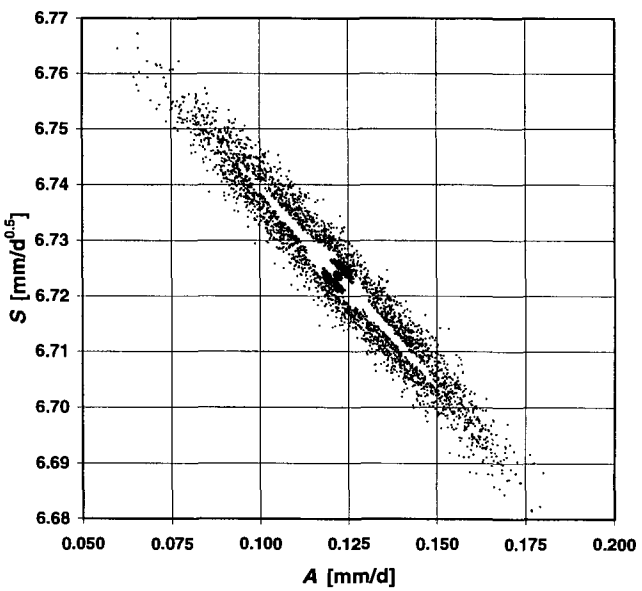

Fig. 4. Plot of 5000 (A, S) optima (Eq. [3]) obtained by fitting the Philip (1957b) model to the 20-h clay data with large imposed measurement error.

The average locally estimated parameter correlation values (obtained from the off-diagonal terms in **B**) were reasonably close to the respective actual parameter correlation only for the two- and three-parameter models and the 20-h sandy loam data. Only in these cases would it be possible to use the complete covariance matrix to more accurately estimate prediction uncertainty. Therefore, considering that the applicability of the estimated covariance matrix cannot be known from a single curve fit, one will in general be limited to using only the independent parameter uncertainties, which will typically result in an overestimated (i.e., conservative) prediction uncertainty.

Time Dependence of Parameters

Time invariance of the parameters is desirable for any model that is to be used for predictive purposes. For each model, Table 6 shows the ratio between the cumulative infiltration values at 20 h as predicted by using the optimized parameters from the 5- and 20-h reference curves. As this ratio approaches unity, the fitted parameters using the short time measurements can be used to predict infiltration for longer times.

As all considered models are simplifications of the true solution to the infiltration problem, perfect time invariance is not to be expected. Indeed, Haverkamp et al. (1988) showed that the parameters of the GA,

Table 6. Ratio between cumulative infiltration I at 20 h predicted from 5-h optimized parameters, and I predicted from 20-h optimized parameters, using reference data.

Model	Clay	Sandy loam
Green and Ampt	1.0029	0.9752
Philip	1.0064	0.9674
Mezencev	0.9998	0.9746
Parlange et al.	1.0007	1.0027
Swartzendruber	1.0006	0.9931
Barry et al.	1.0018	0.9921

Table 7. Optimized hydraulic conductivity for reference data compared with saturated hydraulic conductivity used in the respective finite-element simulation.

Model	Clay		Sandy loam	
	5 h	20 h	5 h	20 h
	mm d^{-1}			
Green and Ampt	0.26611	0.27014	57.758	65.261
Parlange et al.	0.36504	0.35885	93.125	91.253
Swartzendruber	0.13631	0.32098	77.702	82.469
Barry et al.	0.79891	0.79762	80.971	88.632
K_s used in simulation	0.82008		84.298	

Table 8. Optimized sorptivity for reference data compared to theoretical sorptivity.

Model	Clay		Sandy loam	
	5 h	20 h	5 h	20 h
	mm $d^{-0.5}$			
Green and Ampt	6.7053	6.6825	85.571	83.256
Philip	6.7205	6.7243	85.230	81.852
Parlange et al.	6.7205	6.7243	86.254	86.065
Swartzendruber	6.7205	6.7243	86.368	86.937
Theoretical S	6.7281		86.292	
Barry et al.	6.2537	6.2613	78.399	78.172
Theoretical S, no ponding	6.2272		77.754	

PH, and ME models are time dependent. However, the results here suggest that in case of the clay soil, parameters obtained from fitting 5-h data can adequately describe infiltration at least up to 20 h when using any of the considered models. For the sandy loam soil, the PA, SW, and BA models were noticeably less time dependent than the other models, confirming a closer approximation of the true solution by these nonempirical models.

Estimation of Physical Parameters

Hydraulic Conductivity

Table 7 shows a comparison of the K_s values used in the simulations and the optimized parameter for each of the four models, using the reference infiltration data. Of the four models, the BA model reproduced K_s most accurately (to within ≈5%). Overall, the three-parameter PA and SW models arrived at values closer to the original K_s than the GA model. Even for the PA and SW models, however, the results for the clay soil suggest that optimized K_s values should, in general, be viewed as estimates within a factor of two to three. It is reasonable to assume that the 20-h sandy loam data more closely approach steady state than the 20-h clay data. The results in Table 7 then seem to indicate that only if the measurement period comes sufficiently close to steady state can an accurate K_s estimate be expected if the PA and SW models are used for fitting without any prior knowledge.

Sorptivity

Theoretical S values are reported in Table 8 together with the optimized values for the five nonempirical models. In isolating S for the GA and BA models, the fitted K_1 values of Table 7 were used, for BA together with values for h_s (0.05 m for both soils) and $\Delta\theta$ (0.0761 and 0.1582 m^3 m^{-3} for the clay and sandy loam soils, respectively) corresponding with parameters used in the numerical simulations. For all considered models, the theoretical S values matched well with those predicted from fitting (to within ≈5%). Again, the most accurate match was obtained by the BA model (<1% difference). Since the sorptivity represents several soil characteristics simultaneously, this result supports the physical applicability of these models in general; however, the degree of agreement of individual components of S may vary between models.

Computing Efficiency

As shown in Table 9, differences in the number of necessary objective-function calls between models with equal numbers of parameters were small. However, the two nonexplicit models (GA and PA) required computational effort that was one to two orders of magnitude higher than for the other infiltration models.

CONCLUSIONS

Seven infiltration models were tested for their ability to fit simulated infiltration data. The empirical three-parameter HO model consistently resulted in the worst fits in terms of final rms and was discarded because of strong model bias. The PA, SW, and BA models provided the best fits. The fitted parameters of these nonempirical infiltration models also were the least time-dependent among the considered models.

The most accurate parameter confidence-interval predictions were obtained by the PH and ME models, indicating a relatively low nonlinearity associated with their parameters. The confidence-interval predictions for the PA and SW models were accurate for the infiltration data that most closely approached steady state (20 h, sandy loam). Extending the measurement period to-

Table 9. Average number of objective-function calls for small (sm), medium (md), and large (lg) imposed errors (σ_E).

Model	Clay						Sandy loam					
	5 h			20 h			5 h			20 h		
	sm	md	lg	sm	md	lg	sm	md	lg	sm	md	lg
Green and Ampt†	11.4	11.3	11.1	10.5	10.6	9.8	11.9	11.8	11.7	5.7	7.9	8.7
Philip	11.0	11.3	11.7	9.7	9.7	9.7	10.9	11.0	11.0	5.2	7.4	8.5
Mezencev	17.9	18.1	18.3	15.0	15.0	15.0	17.8	18.0	18.3	11.4	14.0	14.5
Parlange et al.†	22.7	24.7	24.8	14.1	14.1	14.0	22.0	21.5	20.1	16.0	16.0	16.0
Swartzendruber	16.1	15.4	15.5	12.8	12.7	12.7	21.1	21.9	22.1	15.5	15.7	15.8
Barry et al.	24.1	23.6	24.1	17.2	17.3	17.6	30.5	29.2	28.9	27.3	25.9	24.9

† Model requires iterative solutions.

ward the steady-state range also increased parameter confidence itself, i.e., the minima in the objective functions became better defined, for all models except BA.

The nonempirical GA, PA, SW, and BA models provided practically useful estimates of the saturated hydraulic conductivity parameter. This estimate can be expected to improve for data sets that extend toward the steady-state range as the relative importance of the hydraulic conductivity in describing cumulative infiltration increases with time. The best match of the original K_s was obtained by the BA model. The same model also achieved the best match in S. The values of S predicted by the GA, PH, PA, and SW models were also very close to the theoretical value for the two soils that were studied. Due to the complex definition of this parameter, the usefulness of this agreement will depend on the particular soil characteristic of interest.

While model fitting performance was approximately similar for the PA, SW, and BA models, the computational expense of the PA model was substantially higher due to its inverse formulation. The BA model, while perhaps the most advanced in its theoretical development, was not found ideally suited as a pure fitting model due to nonuniqueness problems caused by the large number of parameters when assuming no prior knowledge. The number of optima in the objective function would probably decrease if the dimensionality of the search space, i.e., the number of fitting parameters, were reduced by fixing parameters at known values. The necessary measurements require additional effort, may be difficult to obtain, and may potentially have substantial uncertainty themselves. Overall, under the conditions imposed in this study, the SW model (Swartzendruber, 1987) was a reasonable compromise considering all selected criteria.

ACKNOWLEDGMENTS

We wish to express our gratitude to Don Nielsen for his insight during numerous discussions in preparation of this paper, and to Peter Raats for some valuable comments in an early review of the manuscript.

REFERENCES

Barry, D.A., J.-Y. Parlange, R. Haverkamp, and P.J. Ross. 1995. Infiltration under ponded conditions: 4. An explicit predictive infiltration formula. Soil Sci. 160:8–17.

Bazaraa, M.S., H.D. Sherali, and C.M. Shetty. 1993. Nonlinear programming: Theory and algorithms. 2nd ed. John Wiley & Sons, New York.

Clausnitzer, V., and J.W. Hopmans. 1995. Nonlinear parameter estimation: LM-OPT, General-purpose optimization code based on the Levenberg–Marquardt algorithm. Version 1.0 for UNIX. Land, Air and Water Resour. Pap. 100032. Univ. of Calif., Davis.

Green, W.A., and G.A. Ampt. 1911. Studies on soils physics: 1. The flow of air and water through soils. J. Agric. Sci. (Cambridge) 4:1–24.

Haverkamp, R., M. Kutílek, J.-Y. Parlange, R. Lendon, and M. Krejca. 1988. Infiltration under ponded conditions: 2. Infiltration equations tested for parameter time-dependence and predictive use. Soil Sci. 145:317–329.

Haverkamp, R., J.-Y. Parlange, J.L. Starr, G. Schmitz, and C. Fuentes. 1990. Infiltration under ponded conditions: 3. A predictive equation based on physical parameters. Soil Sci. 149:292–300.

Horton, R.E. 1940. An approach towards a physical interpretation of infiltration capacity. Soil Sci. Soc. Am. Proc. 5:399–417.

Kool, J.B., and M.Th. van Genuchten. 1991. HYDRUS. One-dimensional variable saturated flow and transport model including hysteresis and root water uptake. U.S. Salinity Lab., Riverside, CA.

Kostiakov, A.N. 1932. On the dynamics of the coefficient of water percolation in soils and on the necessity of studying it from a dynamic point of view for purposes of amelioration. p. 17–21. Trans. Commiss. VI Int. Soc. Soil Sci., Moscow. 1932. Part A.

Kutílek, M., and D.R. Nielsen. 1994. Soil hydrology. Catena-Verlag, Cremlingen, Germany.

Mezencev, V.J. 1948. Theory of formation of the surface runoff. (In Russian.) Meteorol. Gidrol. 3:33–40.

Parlange, J.-Y., R. Haverkamp, and J. Touma. 1985. Infiltration under ponded conditions: 1. Optimal analytical solution and comparison with experimental observations. Soil Sci. 139:305–311.

Parlange, J.-Y., I. Lisle, R.D. Braddock, and R.E. Smith. 1982. The three-parameter infiltration equation. Soil Sci. 133:337–341.

Philip, J.R. 1957a. The theory of infiltration: 1. The infiltration equation and its solution. Soil Sci. 83:345–357.

Philip, J.R. 1957b. The theory of infiltration: 2. The profile at infinity. Soil Sci. 83:435–448.

Philip, J.R. 1957c. The theory of infiltration: 4. Sorptivity and algebraic infiltration equations. Soil Sci. 84:257–264.

Philip, J.R. 1958. The theory of infiltration: 6. Effect of water depth over soil. Soil Sci. 85:278–286.

Philip, J.R. 1987. The infiltration joining problem. Water Resour. Res. 12:2239–2245.

Press, W.H., S.A. Teukolsky, W.T. Vetterling, and B.P. Flannery. 1992. Numerical recipes in C. 2nd ed. Cambridge Univ. Press, Cambridge, England.

Swartzendruber, D. 1987. A quasi-solution of Richards' equation for the downward infiltration of water into soil. Water Resources Res. 23:809–817.

Talsma, T., and J.-Y. Parlange. 1972. One-dimensional vertical infiltration. Aust. J. Soil Res. 10:143.

van Genuchten, M.Th. 1980. A closed-form equation for predicting the hydraulic conductivity of unsaturated soils. Soil Sci. Soc. Am. J. 44:892–898.

Wendroth, O., W. Ehlers, J.W. Hopmans, H. Kage, J. Halbertsma, and J.H.M. Wösten. 1993. Reevaluation of the evaporation method for determining hydraulic functions in unsaturated soils. Soil Sci. Soc. Am. J. 57:1436–1443.

Youngs, E. 1995. The physics of infiltration. Soil Sci. Soc. Am. J. 59:307–313.